Measurement of Correlation-Enhanced Collision Rates

F. Anderegg, D. H. E. Dubin, T. M. O'Neil, and C. F. Driscoll
Department of Physics, University of California at San Diego, La Jolla, California 92093, USA
(Received 23 September 2008; published 6 May 2009)

We measure the perpendicular-to-parallel collision rate $\nu_{\perp\parallel}$ in laser-cooled magnetized ion plasmas, spanning the uncorrelated to correlated regimes. In correlated regimes, we measure collision rates consistent with the "Salpeter correlation enhancement" of roughly $\exp(\Gamma)$, for correlation parameters $\Gamma \lesssim 4$. This enhancement also applies to fusion in dense plasmas such as stars.

DOI: 10.1103/PhysRevLett.102.185001 PACS numbers: 52.27.Jt, 24.10.Pa, 52.20.Hv, 52.27.Gr

This Letter presents the first detailed experimental measurements of the Salpeter enhancement factor in a strongly correlated plasma. This factor is predicted to enhance the nuclear reaction rate in dense strongly correlated plasmas, such as those found in giant planet interiors, brown dwarfs, and degenerate stars [1], and recent theory establishes that it also applies to perpendicular-to-parallel collisions in magnetized plasmas [2]. The enhancement is caused by plasma screening of the repulsive Coulomb potential between charges, allowing closer collisions for a given relative energy. The enhancement factor $f(\Gamma)$ is predicted to be large when the plasma correlation parameter $\Gamma \equiv e^2/aT$ is larger than unity, scaling as $f(\Gamma) \sim \exp(\Gamma)$. Here e is the charge on each particle, T is the temperature, and a is the Wigner-Seitz radius defined in terms of density n as $4\pi n a^3/3 = 1$.

Laboratory observation of nuclear reactions in a strongly coupled plasma would require prohibitively high temperature (for measurable reaction rates) and high density (so that $\Gamma > 1$). Instead, we measure the analogous Salpeter enhancement of perp-to-parallel energy equipartition in a cryogenic, strongly magnetized pure ion plasma. Strong magnetization means that the kinetic energy of cyclotron motion is an adiabatic invariant, and perp-to-parallel collisions are strongly suppressed. This occurs when $\bar{\kappa} \equiv \sqrt{2}b/r_c \gg 1$, where $b = e^2/T$ is the distance of closest approach, $r_c = \bar{v}/\Omega_c$ is the mean cyclotron radius, $\bar{v} = \sqrt{T/m}$ is the thermal speed, and $\Omega_c = eB/mc$ is the cyclotron frequency. Cyclotron energy is exchanged with parallel energy only through rare close collisions that break this invariant [3], in direct analogy with nuclear energy liberated through close collisions. The equipartition rate $\nu_{\perp\parallel}$ between perpendicular and parallel temperatures is enhanced by plasma screening in exactly the same way as the nuclear reaction rate in two regimes: the weakly correlated regime $\Gamma \ll 1$ and the strong-screening regime $1 \leq \Gamma \ll \bar{\kappa}^{+2/5}$.

This analogy is surprising because the rates are controlled by very different processes (nuclear reactions versus breaking of an adiabatic invariant) in very different plasmas, for which the densities and temperatures differ by many orders of magnitude. Nevertheless, the enhancement factor $f(\Gamma)$ is the same for both rates because the rates are dominated by close collisions, and the enhancement measures the increase in probability of such close collisions due to plasma screening [2,4]. Furthermore, this factor is a thermal equilibrium quantity [5] predicted for a classical plasma to depend on temperature and density only through the single parameter Γ, so fusing ions in an astrophysical fusion plasma can be modeled by a cryogenic plasma with the same Γ value.

The equipartition rate in a strongly magnetized uncorrelated pure electron plasma has been previously measured, demonstrating suppressed collisionality due to the cyclotron adiabatic invariant, but these measurements were limited to $T \gtrsim 25$ K and $n \lesssim 10^9$ cm^{-3}, giving $\Gamma \lesssim 0.1$ [6]. Pure ion plasmas are routinely laser cooled into the highly correlated crystalline regime [7]. Jensen *et al.* [8] reported enhanced collisionality with impurity ions in a beryllium ion plasma at $T = 8 \times 10^{-7}$ eV and $\Gamma = 170$. The inferred collisionality was roughly 10 orders of magnitude greater than predicted by models neglecting correlations, but these experiments were in a classical pycnonuclear regime [2,4] of $\Gamma > \bar{\kappa}^{+2/5}$, where no theory of $f(\Gamma)$ has been developed.

Here we obtain quantitative collision rates versus temperature and density utilizing pure magnesium ion plasmas in a cylindrical Penning-Malmberg trap with $B_z = 3$ Tesla. The measured equipartition rates extend over the range $1 \lesssim \nu_{\perp\parallel} \lesssim 10^4$ sec^{-1} as the temperature is varied over the range $10^{-5} \lesssim T \lesssim 1$ eV. The collision rates are measured at two densities; strong correlation effects are observed on plasmas with density $n = 2 \times 10^7$ cm^{-3}, giving $\Gamma = 5(n/10^7 \text{ cm}^{-3})^{1/3}(T/10^{-5} \text{ eV})^{-1} \lesssim 14$, and these are compared to less correlated plasmas with $n = 0.12 \times 10^7$ cm^{-3}. The measured rates are consistent with the predicted Salpeter correlation enhancement $f(\Gamma)$, with the comparison limited by systematic spatial variations in the plasma temperature.

The ion trap [9] consists of a series of hollow conducting cylinders of radius $r_w = 2.86$ cm contained in an ultrahigh vacuum $P_N \simeq 10^{-10}$ Torr, giving an ion-neutral collision rate of $\nu_{iN} = 2.5 \times 10^{-3}$ sec$^{-1}(P_N/10^{-10}$ T). The plasma length is $L_p \simeq 10$ cm, and the plasma radius $r_p \simeq 0.4$ cm. The magnesium ions are confined for days with a "rotating wall" technique [10]. For collision rate measurements

 © 2009 The American Physical Society

presented here, the rotating wall is turned off a few hundred milliseconds before performing the measurement, and turned back on after the measurement. The laser-induced fluorescence measurements of density and temperature are performed under the same conditions used for the collision measurements.

The plasma temperature is controlled by a ~4 mm wide cooling laser beam parallel to the magnetic field, illuminating essentially all the ions during one $\mathbf{E} \times \mathbf{B}$ drift rotation, with $f_E \simeq 5$ kHz $(n/10^7\ \mathrm{cm}^{-3})$. The cooling beam is chopped at 250 Hz with a chopper wheel, and the temperature is measured with a separate probe laser beam when the cooling beam is blocked. The cooling beam and the probe beam each come from separate frequency-doubled dye lasers. We use the cyclic ${}^2S_{1/2}^{m_j=-1/2} \rightarrow {}^2P_{3/2}^{m_j=-3/2}$ (280 nm) transition to laser cool the plasma. Both $T_\parallel$ and $T_\perp$ are measured with the probe beam; however, the $T_\perp$ measurement has a substantial rotational broadening for $T < 10^{-4}$ eV, so we use only $T_\parallel$ to characterize the plasma temperature T. The equilibrium plasma temperature profile is broadly uniform near center, but often peaks 2× higher at the plasma edge. Moreover, cooling laser frequency variations cause temperature fluctuations up to 50% at the lowest temperatures.

We use two different techniques to measure the perp-to-parallel collision rate $\nu_{\perp\parallel}$. The first technique directly observes $T_\perp$ and $T_\parallel$ as they relax to a common value, as done in Ref. [11]. The parallel temperature is initially increased by a small oscillating potential applied at one end of the plasma, resulting in $T_\parallel > T_\perp$; once a steady state has been reached, the heating is turned off, and $T_\parallel$ and $T_\perp$ relax to a common temperature. The evolution of $T_\parallel$ and $T_\perp$ is recorded, and the collision rate $\nu_{\perp\parallel}$ is obtained directly from fitting to $(d/dt)T_\perp = -\nu_{\perp\parallel}(T_\perp - T_\parallel)$.

Figure 1 shows the temporal evolution of $T_\parallel$ and $T_\perp$ during this technique. Up to $t = 2$ seconds, the oscillating potential is applied to the end electrode and a steady state is reached, with $T_\parallel = 0.75$ eV and $T_\perp = 0.66$ eV. Here, the heating provided by the oscillating wiggle is balanced by cooling due to the residual background gas. At $t = 2$ seconds, the oscillating wiggle is turned off, $T_\parallel$ and $T_\perp$ relax to a common temperature at a rate $\nu_{\perp 0}$, while cooling due to the neutral background gas. Subtracting $T_\perp$ from $T_\parallel$ removes the need of modeling the cooling due to neutrals: $(d/dt)(T_\parallel - T_\perp) = -\nu_{\perp 0}(T_\parallel - T_\perp)$ where $\nu_{\perp 0} = 3\nu_{\perp\parallel}$. An exponential fit to $T_\parallel - T_\perp$ gives $\nu_{\perp 0} = 6.8\ \mathrm{s}^{-1}$; we plot this measurement on Fig. 4 as $T = \frac{2}{3}T_\perp + \frac{1}{3}T_\parallel = 0.72$ eV and equipartition rate $\nu_{\perp\parallel} = \frac{1}{3}\nu_{\perp 0} = 2.3\ \mathrm{sec}^{-1}$. The direct measurement technique is not practical when $\nu_{\perp\parallel} > 100\ \mathrm{sec}^{-1}$, and it is not accurate for $T < 10^{-4}$ eV, since ion-neutral collisions give a heating rate $dT/dt \sim 0.6 \times 10^{-4}$ eV/ sec which dominates the temperature evolution. We have used the direct measurement technique essentially to confirm the results from the following "heating versus frequency" technique in the range of $T > 10^{-2}$ eV.

The heating versus frequency technique obtains the collision rate $\nu_{\perp\parallel}$ by determining the frequency f_{osc} at which axial compressions give maximal heating [6]. Here the initial plasma temperature is made as spatially uniform as possible, with a cooling laser balancing the background plasma heating due to neutral collisions, trap asymmetries, and electronic noise. A short oscillating burst (3 → 100 cycles) at frequency f_{osc} is applied to a cylindrical electrode at one end of the plasma. The heating due to the burst is maximal when $\nu_{\perp\parallel} = c(\Gamma)2\pi f_{\mathrm{osc}}$. Here, the specific heat has perpendicular and parallel components, giving $c(\Gamma) = c_\parallel c_\perp/(c_\parallel + c_\perp)$, with $c_\perp = 1$ and $c_\parallel = 1/2 + \partial U_{\mathrm{corr}}/\partial T$; the correlation energy U_{corr} is defined by Eq. (4.24) in Ref. [12]. The specific heat increases slowly with correlation, with $c(0) = 1/3$, $c(2) \simeq 0.42$, and $c(10) \simeq 0.52$.

We measure the heating effect of the oscillating burst with a weak probe laser tuned to the resonant transition; the probe beam spans $0.2 \lesssim r \lesssim 0.3$ cm, and the fluorescence is recorded every 8 ms. Figure 2 shows the effect of a 20 cycle resonant burst at 260 Hz on the probe laser signal or a plasma at temperature $T = 3 \times 10^{-5}$ eV: within a few cycles, the fluorescence drops by 30%; after the burst it slowly recovers due to the cooling laser. We adjust the

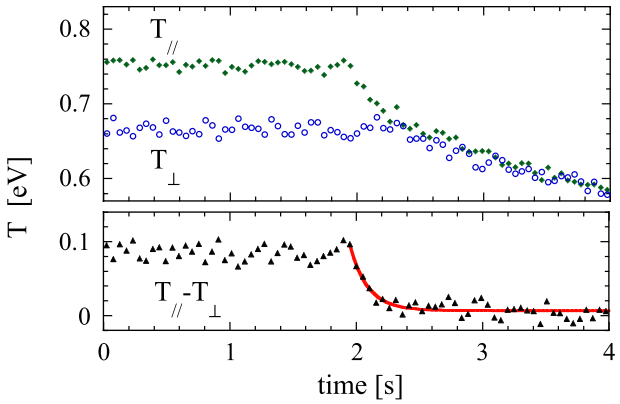

FIG. 1 (color online). Relaxation of temperature anisotropy; the solid curve is the exponential fit.

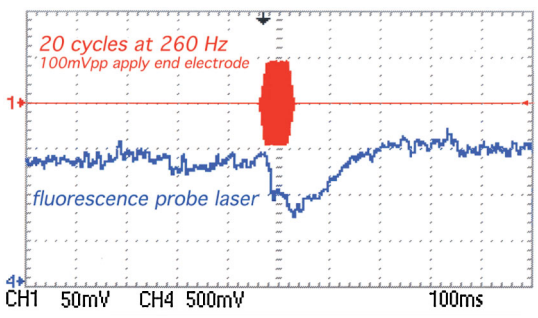

FIG. 2 (color online). Probe laser fluorescence in the presence of a resonant oscillating burst.

oscillation amplitude so that the heating-induced fluorescence drop occurs only at the frequency of maximal heating. Figure 3 shows a typical heating peak, with a width of about 120 Hz out of 3900 Hz; the data were for a plasma with $T = 4 \times 10^{-4}$ eV.

These collisional heating maxima are distinct from heating due to resonant plasma modes. Plasma modes may also be excited by the oscillating burst, if $f_{\rm osc}$ is near a mode resonance. This gives a similar fluorescence signal, since a mode is an efficient way of coupling energy into the plasma and heating the particles. Fortunately, we are able to distinguish modes from collision maxima, since modes have only mild temperature dependence, and modes can be tracked over a wide temperature range. Also the persistent mode oscillations after the oscillating burst has stopped can be detected with other electrodes.

Theory predicts that in the absence of correlation, the perpendicular-to-parallel collision rate for charged particles in a magnetic field is

$$\nu_{\perp\parallel}^{\rm nocorr} = n\bar{v}b^2 I(\bar{\kappa}), \tag{1}$$

where $I(\bar{\kappa})$ represents the effect of the magnetic field on the collision. For $\bar{\kappa} < 1$, Eq. (1) is well approximated [3] by

$$\nu_{\perp\parallel}^{\rm nocorr} = \frac{8\sqrt{\pi}}{15} n\bar{v}b^2[\ln(\sqrt{2}/\bar{\kappa}) + 0.75]. \tag{2}$$

For strong magnetization ($\bar{\kappa} > 1$) a full Monte Carlo calculation is required; the values of $I(\bar{\kappa})$ are given in Tables 1 and 2 and Fig. 1 of Ref. [3]. For example, for $T = 2.5 \times 10^{-5}$ eV the strong magnetization reduces the collision rate by a factor $I(\bar{\kappa}) = 2.7 \times 10^{-6}$ compared to the nonmagnetized case. When the plasma is strongly correlated with $\Gamma \gtrsim 1$, theory predicts that the collision rate is increased [2] by the Salpeter enhancement factor $f(\Gamma)$:

$$\nu_{\perp\parallel} = n\bar{v}b^2 I(\bar{\kappa}) f(\Gamma). \tag{3}$$

The enhancement factor has been evaluated by several authors; Ichimaru [13] predicts that for $\Gamma > 1$, $\ln f(\Gamma) = 1.148\Gamma - 0.009\,44\Gamma\ln\Gamma - 0.000\,168\Gamma(\ln\Gamma)^2$. Equation (3) is only valid for $\Gamma < \bar{\kappa}^{+2/5}$; for our higher density data experiment this limits the range of applicability of the theory to $\Gamma < 20$. When $\Gamma > \bar{\kappa}^{+2/5}$ the plasma enters a classical pycnonuclear regime [2,4] where equipartition is driven primarily by collective effects, and there is as yet no detailed theory for $\nu_{\perp\parallel}$.

The measured perp-to-parallel collision rate is plotted in Fig. 4 for two densities; at the lower density the plasma is never strongly correlated. The solid curves are the result of Eq. (1) using $I(\bar{\kappa})$ calculated in Ref. [3]; the dashed line curves are from Eq. (3) with $f(\Gamma)$ given from Ref. [13]. The correlation parameter Γ is also plotted for both densities. For the "high-temperature" part of the plot ($\bar{\kappa} < 1$) the collision rate varies as expected from Eq. (2) with $\nu_{\perp\parallel} \propto T^{-3/2}$. In the low temperature, strongly magnetized regime ($\bar{\kappa} > 1$), the collision rate decreases rapidly as T is reduced, because the adiabatic invariance of cyclotron energy suppresses equipartition [3,6]. At its peak, the collision rate is about 10^4 sec^{-1} compared to a plasma frequency $f_p = 191$ kHz.

The $n_7 = 2$ data at low temperatures have $\Gamma > 1$, and the measured collisionality is enhanced by many decades over theory neglecting correlations, consistent with the Salpeter correlation enhancement $f(\Gamma)$. To separate the correlation enhancement from the strong magnetization suppression, a set of low density data ($n_7 = 0.12$) is also presented; here theory predicts little difference between the cases with or without correlation, and theory is in close agreement with the measurements. The two data sets differ mainly in their density (and therefore correlations); the neutral pressure, impurity ions, and magnetic field inhomogeneity are the same. Also, the low density data demonstrate that the collision rate in cold plasmas can be correctly measured down to 1 sec^{-1}, setting an upper limit on extraneous collisional effects.

For temperatures $T \geq 1.5 \times 10^{-5}$ eV, the data of Fig. 4 are well described for both densities by Eq. (3). At the lowest temperatures, our measurement uncertainty comes from systematic radial temperature nonuniformities, and

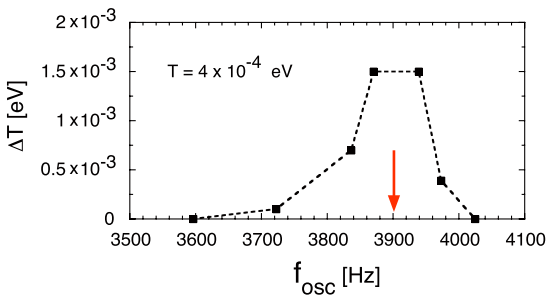

FIG. 3 (color online). Temperature increase resulting from an oscillating burst at $f_{\rm osc}$.

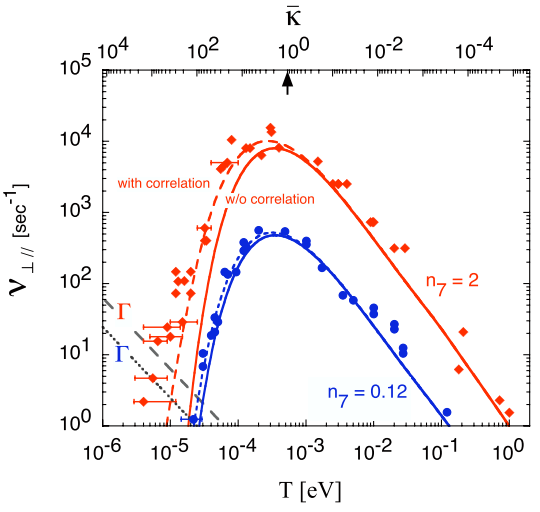

FIG. 4 (color online). Measured collision rate for two densities compared to theory with and without correlations. The correlation parameter Γ is a pure number to be read on the same vertical scale.

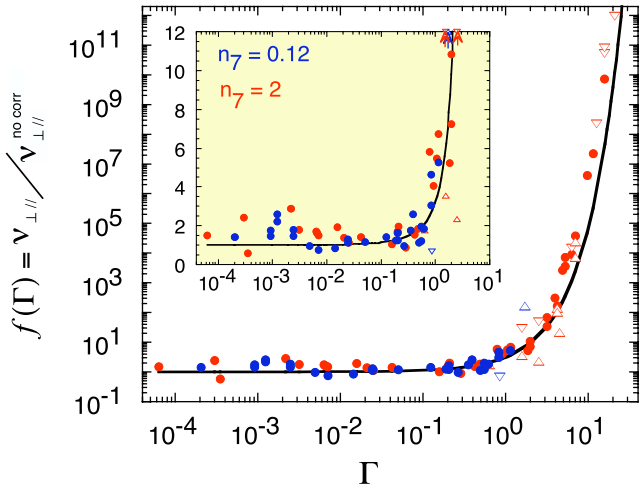

FIG. 5 (color online). Correlation enhancement of the collision rate versus the correlation parameter Γ.

from temporal variations in laser cooling. The data points represent a density-weighted spatial temperature average, and 8 representative error bars are shown. The error bars span the estimated extrema of $T(r)$, with the outer edge being systematically hotter. The collisional heating is inherently spatially averaged, and may also include undiagnosed spatial heat transport effects.

Figure 5 shows the measured $\nu_{\perp\parallel}$ collision rates of Fig. 4 divided by the theory prediction neglecting correlations [Eq. (1)], that is, the Salpeter enhancement $f(\Gamma)$. The enhancement varies exponentially with correlation, as $\nu_{\perp\parallel} \simeq \exp(\Gamma)\nu_{\perp\parallel}^{\text{nocorr}}$, in agreement with Eq. (3) up to $\Gamma \sim 4$. The experimental uncertainty in T translates into uncertainty in Γ and larger uncertainty in $f(\Gamma)$, through $\nu_{\perp\parallel}^{\text{nocorr}}$. For clarity, only the lower and upper temperature ends of the 8 error bars in Fig. 4 are plotted, as down-triangles and up-triangles, respectively. The solid line on Fig. 5 is Eq. (3) with no adjustable parameters, using $f(\Gamma)$ from Ref. [13]. The theories of Ogata [14] and DeWitt and Slattery [15] are undistinguishable from the solid line on this scale. The insert shows the enhancement on a linear scale for $\Gamma < 3$; the arrows pointing up indicate open triangles above the maximum of the linear scale. It is remarkable that the data from both densities lie on the same curve, suggesting that the enhancement depends on Γ, becoming measurable for $\Gamma > 1$. For $\Gamma < 4$, theory describes the data closely. For $\Gamma > 4$, the theory prediction is at the "high-temperature" side of the systematic error bar, suggesting that equipartition in the hotter plasma edge predominates, even though the diagnostic laser is more centrally located. Spatial heat transport must be modeled to fully characterize the energy equipartition; in other experiments with extreme differences between $T_\perp$ and $T_\parallel$, the equipartition may even propagate spatially as a "burn front" [4]. We also note that the largest measured Γ values are on the edge of the pycnonuclear regime where the theory for $f(\Gamma)$ breaks down; however, this should lead to a reduction in the enhancement factor, not an increase [2,4].

To our knowledge, this is the first quantitative experimental measurement of strong-screening enhancement of the $\nu_{\perp\parallel}$ collision rate. The data are consistent with the standard "Debye shielding" theory of the Salpeter correlation enhancement for correlations up to $\Gamma \lesssim 4$. The same enhancement should apply to fusion in dense neutral plasmas such as stars.

This work is supported by NSF/DOE Grant No. PHY-0613740 and by National Science Foundation Grant No. PHY-0354979. We thank Dr. J. J. Bollinger for many valuable discussions on laser-cooled ion plasmas, and C. J. Lee for his assistance in collecting some of the data.

[1] E. E. Salpeter and H. M. Van Horn, Astrophys. J. **155**, 183 (1969); L. R. Gasques *et al.*, Phys. Rev. C **72**, 025806 (2005).
[2] D. H. E. Dubin, Phys. Rev. Lett. **94**, 025002 (2005).
[3] M. E. Glinsky, T. M. O'Neil, M. N. Rosenbluth, K. Tsuruta, and S. Ichimaru, Phys. Fluids B **4**, 1156 (1992).
[4] D. H. E. Dubin, Phys. Plasmas **15**, 055 705 (2008); F. Anderegg, D. H. E. Dubin, C. F. Driscoll, and T. M. O'Neil, Bull. Am. Phys. Soc. **51**, 249 (2006); D. H. E. Dubin, Bull. Am. Phys. Soc. **52**, 190 (2007).
[5] A. Alastvey and B. Jancovici, Astrophys. J. **226**, 1034 (1978).
[6] B. R. Beck, J. Fajans, and J. H. Malmberg, Phys. Plasmas **3**, 1250 (1996); B. R. Beck, J. Fajans, and J. H. Malmberg, Phys. Rev. Lett. **68**, 317 (1992).
[7] J. J. Bollinger, T. B. Mitchell, X.-P. Huang, W. M. Itano, J. N. Tan, B. M. Jelenkovic, and D. J. Wineland, Phys. Plasmas **7**, 7 (2000).
[8] M. J. Jensen, T. Hasegawa, J. J. Bollinger, and D. H. E. Dubin, Phys. Rev. Lett. **94**, 025001 (2005).
[9] F. Anderegg, X.-P. Huang, E. Sarid, and C. F. Driscoll, Rev. Sci. Instrum. **68**, 2367 (1997).
[10] X.-P. Huang, F. Anderegg, E. M. Hollmann, C. F. Driscoll, and T. M. O'Neil, Phys. Rev. Lett. **78**, 875 (1997); F. Anderegg, E. M. Hollmann, and C. F. Driscoll, Phys. Rev. Lett. **81**, 4875 (1998); E. M. Hollmann, F. Anderegg, and C. F. Driscoll, Phys. Plasmas **7**, 2776 (2000).
[11] F. Anderegg, X.-P. Huang, C. F. Driscoll, E. M. Hollmann, T. M. O'Neil, and D. H. E. Dubin, Phys. Rev. Lett. **78**, 2128 (1997); F. Anderegg, X.-P. Huang, E. M. Hollmann, C. F. Driscoll, T. M. O'Neil, and D. H. E. Dubin, Phys. Plasmas **4**, 1552 (1997).
[12] D. H. E. Dubin and T. M. O'Neil, Rev. Mod. Phys. **71**, 87 (1999).
[13] S. Ichimaru, Rev. Mod. Phys. **65**, 255 (1993).
[14] S. Ogata, Astrophys. J. **481**, 883 (1997).
[15] H. DeWitt and W. Slattery, Contrib. Plasma Phys. **39**, 97 (1999).